A model for the biochemical degradation of inosine monophosphate in hake (*Merluccius merluccius*)

C. Vilas[a], A.A. Alonso[a,*], J.R. Herrera[b], A. García-Blanco[c], M.R. García[a]

[a]*Bioprocess Engineering Group. IIM-CSIC. c/ Eduardo Cabello,6. 36208 Vigo, Spain*
[b]*Microbiology and Technology of Marine Products, IIM-CSIC, c/ Eduardo Cabello 6, 36208, Vigo, Spain*
[c]*Scientific instrumentation, IIM-CSIC, c/ Eduardo Cabello 6, 36208, Vigo, Spain*

Abstract

ATP-derived products are typically used as early indicators of fish quality loss during storage. In this work, we explore different biochemical routes that are potentially relevant in contributing to nucleotide degradation in hake (*Merluccius merluccius*). A major motivation of this study is to get more insight on the biochemical degradation mechanisms of nucleotide catabolites in hake muscle at fish storage and transport conditions. This requires the identification of its relevant pathways.

To that purpose, different degradation routes proposed in the literature are considered and a mathematical model for the degradation process is derived. First order kinetics are assumed for all the reactions and temperature dependence is taken into account through the Arrhenius equation. Unknown model parameters, namely activation energies and pre-exponential Arrhenius coefficients, are estimated via fitting to experimental data. From the estimation results, relevant routes are identified. The kinetic study is performed on sterile fish juice to avoid coupling with microbial degradation mechanisms or possible interferences of the food matrix that might hide biochemical interactions.

The proposed scheme adequately describes biochemical changes in nucleotide catabolites under variable temperature profiles. It also reveals a pathway which at least seems relevant for nucleotide degradation in hake.

Keywords: Fish freshness, Parameter estimation, Nucleotide degradation, Dynamic model, Biochemical pathways

1. Introduction

The degradation of nucleotide catabolites has been typically used as an early indicator of fish freshness [39, 44, 33], which usually serves as an attribute of quality during fish storage [43, 10]. Such compounds are the result of adenosine triphosphate (ATP) degradation. Within the first 24-48 hours after fish has died, ATP quickly transforms into inosine 5′-monophosphate (IMP), via adenosine diphosphate (ADP) and adenosine monophosphate (AMP) degradation [24, 27]. In the order of days to weeks, IMP degradation continues on a cascade reaction that produces inosine (Ino) and hypoxanthine (Hx), which is further decomposed into other compounds such as xanthine and uric acid [22, 23]. IMP contributes to the *umami* flavour, related to the pleasant sweet and meaty flavors in fresh fish [25, 26, 21], whereas Hx is responsible of unpleasant bitterness [41, 19, 29]. One of the indexes most widely employed to evaluate freshness is the K-index, which is defined as the ratio of the sum of Ino and Hx to the sum of all ATP degradation products [39].

Understanding the biochemical degradation mechanisms is of paramount importance to predict quality loss at the early stages of postmortem fish, and to improve, in this way, storage or distribution conditions. The evolution of the K-value from experimental measurements of the ATP-derived products as well as its relation to fish quality and shelf-life have been extensively studied - see, for instance [39, 9, 2, 34, 7, 31, 38, 49, 40, 21] and references therein-. However, despite all these works, studies focusing on the degradation kinetics are scarce [48]. To the best of our knowledge, the first mechanistic approach to describe nucleotide degradation was reported in [8] who performed the study in an enzyme-free aqueous solution. As complete ATP conversion into IMP occurs during the first 24/48 hours after fish death, degradation can be assumed to be initiated with IMP, particularly at retail level, what results into the following pathway:

$$\text{IMP} \rightarrow \text{Ino} \rightarrow \text{Hx} \rightarrow \text{Products}$$

Firstly, IMP is transformed to Ino by the action of a 5′-nucleotidase or some phosphatases [24, 14, 23, 28]. Then, either purine nucleoside phosphorylase or inosine nucleosidase convert inosine to hypoxanthine, which is in turn degraded by xanthine oxidase into xanthine and uric acid. In this scheme, kinetics are assumed to be first order, with reaction rate coefficients exhibiting an Arrhenius temperature dependence. Some extensions of this degradation kinetics pathway have been proposed in [22, 23]. The model incorporates mechanisms to account for possible losses of compounds by leaching (or diffusion) through the food matrix and includes the effect of

*Corresponding author. Ph: +34 986 231 930 Ext. 251
Email addresses: carlosvf@iim.csic.es (C. Vilas), antonio@iim.csic.es (A.A. Alonso), juanherrera@iim.csic.es (J.R. Herrera), anagarci@iim.csic.es (A. García-Blanco), miriamr@iim.csic.es (M.R. García)

bacteria in the transformation of Ino into Hx. A version of this model has been employed to predict nucleotide degradation in rainbow trout (*Oncorhynchus mykiss*) with very satisfactory results [22]. In [23], kinetic parameters were estimated from data available in the literature, covering a wide range of species stored in ice and captured in different seasons and places. The model was able to fit most of the data, although general conclusions could not be drawn due to the large variability of the estimated parameters among species.

The degradation of IMP in fish muscle may involve further pathways in which enzyme activity largely varies among species [24]. This motivated several authors to propose different degradation routes not considered in the classical catabolism of nucleotides. In this regard, [24] presented a degradation scheme for ATP, which included the most relevant routes and some of minor importance. The scheme employed in Howgate [22, 23] is a simplified version of this one. Additional routes, not considered in [24] were described in the literature. For instance, [16] pointed out that IMP might directly yield Hx and ribose-5-phosphate; whereas other authors suggested the possibility of equilibrium between IMP and Ino [14] as well as Ino and Hx [42, 14, 32]. IMP has also been found to give rise to xanthosine monophosphate (XMP) via IMP dehydrogenase [32, 36]. In addition, salvage pathways can give rise to IMP from both Ino and Hx via a nucleoside kinase and a phosphoribosyltransferase, respectively [36].

In this work, the above mentioned biochemical routes, potentially relevant in contributing to nucleotide degradation in fish, are explored. A mathematical model is derived for the degradation process assuming first order reaction dynamics and Arrhenius like temperature dependence for the reaction rates. The values of the Arrhenius parameters, namely pre-exponential factors and activation energies, are computed by fitting the model solution to the experimental data. This also allows us to identify the relevant routes and neglect those of minor importance. Sterile fish juice, obtained from the muscle, is used as the experimental system. In this way, possible overlapping with microbial degradation mechanisms for the transformation of Ino to yield Hx or nucleotide catabolites loss by leaching are avoided, allowing us to focus on the biochemical interactions.

This study provides evidence on the existence of alternative biochemical routes of IMP degradation, relevant at least for hake at storage conditions, that have not been considered in previous mathematical models. In this regard, the study reveals an alternative biochemical route that directly converts IMP in Hx and other degradation products. Finally, it should be noted that, although the model that we propose includes only biochemical pathways, it can be combined in a modular way with bacterial growth models [e.g. 6, 13] to account for bacterial conversion of Ino to Hx or with models that account for mass transfer in the food matrix [23].

2. Materials and methods

2.1. Experimental methods

2.1.1. Preparation of juice from fish muscle

A total of 13 fresh gutted medium-sized hake (*Merluccius merluccius*) (1.2 kg to 1.4 kg each) caught in Galician waters were purchased from the retail market in Vigo (Spain) during the first 24 h after death. Hake was transferred to the laboratory within 30 min in expanded polysterene boxes with ice. Once in the lab, fish were skinned and filleted, and fillets were thoroughly ground by using a Dito Sama K35 cutter mixer at high speed for 10 s. Ground muscle was cooled at 4 °C and subsequently centrifuged at 7500 g for 20 min at 4 °C.

Supernatants were collected and subject to a second centrifugation at 40.000 g for 15 min at 4 °C to remove small solids and particulate matter still present. Clear supernatants were then collected and vacuum-filtered sequentially through a 0.45 μm pore size and then a 0.22 μm pore size cellulose acetate membrane filter under sterile conditions with the aim to remove all bacteria present. Sterility was tested by spreading 0.5 mL of extracts on plate count agar (PCA) followed by incubation during 5 days at 17 °C. This was performed prior to and repeatedly during storage of samples. It is important to mention that the organelles released after cell disruption during the preparation procedure should not be removed by filtration since they are smaller than the pore size of filters. In this way, it is reasonable to assume that all relevant enzymes responsible of nucleotide degradation were present in the aqueous solution.

2.1.2. Storage trials

Fish muscle juice was diluted in mili-Q sterile water at a ratio 1:1 and distributed in 2 ml-aliquots into glass test tubes. Tubes were divided into three batches which were stored under typical range of storage/transport conditions, including situations that involve the interruption of the cold chain storage. In this regard, a first batch was stored at 2 °C for 30 days. A second batch was stored at 5 °C for 16 days followed by 14 days at 16 °C. The last batch was stored for 20 °C for 6 days followed by 24 days at 10 °C. A thermocouple was placed in each cabinet to continuously record the temperature throughout the storage period. Three tubes were taken out of cabinets on working days during storage for nucleotide catabolites analysis.

2.1.3. Nucleotide catabolites analysis

The analysis is based on the method described in [35]. A 1.5 ml-aliquot of cold 0.6 M perchloric acid was added onto each tube and thoroughly mixed by vortexing for 10 s in an ice-water bath. Mixtures were stored at -20 °C for 10 min and then centrifuged at 1000 g for 10 min at 4 °C. Supernatants were collected and immediately potassium hydroxide was added up to reach a pH between 6.5-6.8. Once neutralized, homogenates were kept for 30 min in an ice-water bath for precipitation of potassium perchlorate and subsequently filtered through a wet Whatman No. 1 filter paper. Filtrates were stored at -80 °C until chromatographic analysis were carried out.

Nucleotide catabolites analysis was carried out by reverse-phase high-performance liquid chromatography (RP-HPLC) by using an Agilent Model 1200 Series chromatograph (Agilent, Waldbronn, Germany) equipped with a variable wavelenght detector (Agilent UV-VIS G1314B) and a binary pump (Agilent G 1312A). A Spherisorb ODS2 (C18) column (5 μm particle size, 4.6 × 250 mm) (Waters, Ireland) was installed inside a ther-

mostated compartment (Agilent TCC G1316A) for use at a temperature of 22 °C.

Standards for ATP-derived products (adenosine 5′-triphosphate (ATP), adenosine 5′-diphosphate (ADP), adenosine 5′-monophosphate (AMP), inosine 5′-monophosphate (IMP), inosine (Ino) and hypoxanthine (Hx)) as well as potassium phosphate salts were purchased from Sigma-Aldrich Chemical Company (Poole, Dorset, UK).

Chromatograpphic separation was achieved by using gradient elution with phosphate buffer (mobile phase A) and acetonitrile (mobile phase B). Chromatographic condition for analysis are shown in Table 1. Mobile phase A

Time	Mobile Phase A (%)	Mobile Phase B (%)	Flow rate (ml min^{-1})	Maximum Pressure (bar)
0.00	100.0	0.0	1.00	400
8.00	97.5	2.5	1.00	400
10.00	95.0	5.0	1.00	400
12.00	70.0	30.0	1.00	400
17.00	0.0	100.0	1.00	400
20.00	100.0	0.0	1.00	400

Table 1: HPLC gradient profile used for separation of nucleotide catabolites.

consisted of a 50:50 mixture of 0.04 M potassium dihydrogen phosphate (KH2PO4) and 0.06 M potassium monohydrogen phosphate (K2HPO4) in Milli-Q water (HPLC grade) adjusted to pH 7.0 with 0.1 M potassium hydroxide. Solutions were prepared on a daily basis and filtered through GH Polypro (hydrophilic polypropylene) membrane disc filters (0.45 μm pore size) (Gelman Sciences, Northampton, UK). Acetonitrile (HPLC grade) (Merk, Darmstadt, Germany) was used as mobile phase B. Injection volume was 20 μL and detection was monitored at 254 nm. Total run time was 20 min.

A calibration curve was obtained for each nucleotide catabolite within the range 0.1-1-0 mM. Correlation coefficients between peak area and concentration as well as coefficients of variation were determined for each nucleotide catabolite after injection of 5 replicates of each standard solution.

3. Model description and mathematical tools for parameter estimation

As mentioned in the introduction, degradation of IMP in fish involves a series of complex pathways, what motivated several authors to propose alternative degradation routes. Such routes, indicated in the introduction, are schematically represented in Figure 1.

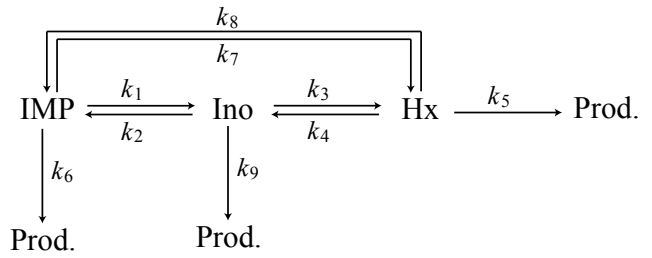

Figure 1: Postmortem degradation scheme of IMP in fresh fish with alternative degradation pathways reported in the literature.

Assuming that enzymatic degradation of IMP, Ino and Hx follow first order kinetics, the mathematical model for the scheme in Figure 1 is of the form:

$$\frac{\mathrm{dIMP}}{\mathrm{d}t} = -(k_1 + k_6 + k_7)\mathrm{IMP} + k_2\mathrm{Ino} + k_8\mathrm{Hx} \quad (1)$$

$$\frac{\mathrm{dIno}}{\mathrm{d}t} = -(k_2 + k_3 + k_9)\mathrm{Ino} + k_1\mathrm{IMP} + k_4\mathrm{Hx} \quad (2)$$

$$\frac{\mathrm{dHx}}{\mathrm{d}t} = -(k_4 + k_5 + k_8)\mathrm{Hx} + k_3\mathrm{Ino} + k_7\mathrm{IMP} \quad (3)$$

where k_i with $i = 1, ..., 9$ are the reaction rate coefficients whose dependency on the storage temperature is described by the Arrhenius equation:

$$k_i = A_i \exp\left(-\frac{E_{a,i}}{RT}\right); \quad (4)$$

with $E_{a,i}$ and A_i being, respectively, the activation energy and the pre-exponential factor of each reaction i; $R = 1.987$ kcal K^{-1} kmol^{-1} is the universal gas constant and T in K is the storage temperature.

In this work, the solution of Eqns (1)-(3) is numerically computed using the CVODEs solver [20], which includes the well-established *Backward Differentiation Formula* (BDF) as an integration method.

In order to equip the model with predictive capabilities, unknown model parameters must be estimated from experimental data. Parameter estimation is formulated as an optimization problem where the objective is to obtain the parameter values that minimize the distance between model predictions and experimental data [46]. A good measure of such distance can be obtained through the log-likelihood function which, for normally and independent distribution data, corresponds to [47]:

$$J(\theta) = -\frac{1}{2}\sum_{k=1}^{n_c}\sum_{i=1}^{n_{x_k}}\left[\log(2\pi) + \log\left(\sigma^2_{x_{k,i}}\right) + \left(\frac{x_{k,i}(\theta) - x^{exp}_{k,i}}{\sigma_{x_{k,i}}}\right)^2\right] \quad (5)$$

with x_k being the concentration of each of the considered compounds (i.e. x_1 = IMP, x_2 = Ino and x_3 = Hx) and n_{x_k} being the number of sampling points per component (for instance n_{x_1} is the number of time measurements for IMP). θ corresponds with the unknown model parameters to be estimated. $x_{k,i}(\theta)$ and $x^{exp}_{k,i}$ represent the concentration of compound x_k at time t_i computed from the model and measured in the experiments, respectively. Finally, $\sigma_{x_{k,i}}$ corresponds with the variability of measurement x_k at time t_i. It is clear that function $J(\theta)$ depends on the nature of data noise and data variability, and gives more relevance to those data with lower variability.

Maximum likelihood estimates correspond with the maximum of Eqn (5). Maximization of $J(\theta)$ (or equivalently minimization of $-J(\theta)$) subject to the model dynamics (1)-(3) is computed using a numerical solver. Optimization for most solvers involves the following steps: i) assign values to the unknown parameters within the allowed range; ii) solve the model equations; iii) compute $J(\theta)$ using the model solution and experimental measurements at times t_i; iv) obtain new candidates for θ using $J(\theta)$ and previous values of θ; v) repeat steps 1-4 till convergence.

It is often the case that function $J(\theta)$ has several minima (suboptimal solutions). Details about the different methodologies to numerically minimize a given function can be found elsewhere in the literature -see, for instance, [11, 12, 37] and references therein-. Hybrid optimization methods, which profit from the advantages of global and local approaches, are preferred to efficiently find the best solution [4]. In this work, the toolbox AMIGO2 [5] is used to find the minimum of $J(\theta)$.

The unknown parameters to be estimated in this work are those of the Arrhenius equation (4), i.e. activation energies and pre-exponential factors.

It should be noted that solving Eqns (1)-(3) requires the value of the nucleotide catabolites at $t = 0$ (*initial conditions*), i.e. IMP($t = 0$), Ino($t = 0$) and Hx($t = 0$). In this work, $t = 0$ corresponds with the beginning of fish juice storage trial, i.e. when the first experimental measurement is taken. One way to proceed is to use such measurement as the initial condition. However, this approach is very sensitive to measurement errors as divergences in the initial conditions may lead to over- or under-estimation of the degradation kinetics. To avoid this situation, typical in data subject to variability or noise, initial conditions are also estimated. In other words, the initial measurement is treated in the optimization as any other experimental measurement. This approach has been followed in other works [22, 13].

4. Results and discussion

As discussed in the introduction, 24-48 hours after death IMP is the only nucleotide present in most fish species because of the fast degradation of ATP into IMP. [22] pointed out that small amounts of ADP might be released during the extraction procedure of nucleotides. However, this ADP is likely to be bound to myofibrillar proteins which, in our case, were removed by centrifugation. Furthermore, this ADP does not take part in the degradation of free nucleotides so it would have no relevance in the present study. Analysis performed in this work, which were carried out around 24 hours after fish death, confirmed that ATP, ADP and AMP were absent in the fish juice. The remaining compounds of interest (IMP, Ino and Hx) were measured along the duration of the experiments.

In order to prevent the conversion of Ino into Hx due to bacterial action [41, 22], and to avoid loss of nucleotide catabolites by leaching [23] we use sterile-filtered fish muscle juice as the experimental system. Such juice was separated in three batches (three experiments) which were stored under the experimental conditions described in section 2.1.2. [45, 18, 17] suggest that experiments with variable storage conditions are more informative for model identification purposes than experiments with constant storage conditions. Therefore, two of the experiments were carried out using a step profile in the storage temperature. Mean values of the experimental data for each sampling time as well as their corresponding standard deviations are presented in Tables A.4–A.6 in Appendix A. Each of the values, mean and std, were computed from three samples. Points with standard deviation larger than 0.5 mM were removed from the computations. Tables also show the sampling times and the measured storage temperature.

The unknown model parameters to be estimated from this data set are the Arrhenius coefficients ($E_{a,i}$ and A_i) for all the reactions as well as initial conditions for IMP. Experimental measurements showed that the concentrations of Ino and Hx at the beginning of the experiments are zero or close to zero so they will not be estimated from data. All the experiments started from the same initial conditions.

The values obtained during the estimation of the unknown parameters are presented in Table 2. Activation

Parameter	Value	Units	k [d^{-1}] at 20 °C
$E_{a,1}$	2.77×10^4	kcal kmol^{-1}	$k_1 = 0.27$
A_1	1.15×10^{20}	d^{-1}	
$E_{a,2}$	1.80×10^5	kcal kmol^{-1}	$k_2 = 2.09 \times 10^{-63}$
A_2	6.87×10^{71}	d^{-1}	
$E_{a,3}$	2.18×10^4	kcal kmol^{-1}	$k_3 = 0.43$
A_3	7.63×10^{15}	d^{-1}	
$E_{a,4}$	1.98×10^5	kcal kmol^{-1}	$k_4 = 2.06 \times 10^{-76}$
A_4	1.00×10^{72}	d^{-1}	
$E_{a,5}$	2.00×10^5	kcal kmol^{-1}	$k_5 = 5.35 \times 10^{-78}$
A_5	5.99×10^{71}	d^{-1}	
$E_{a,6}$	2.56×10^4	kcal kmol^{-1}	$k_6 = 0.22$
A_6	2.29×10^{18}	d^{-1}	
$E_{a,7}$	1.81×10^4	kcal kmol^{-1}	$k_7 = 0.15$
A_7	4.84×10^{12}	d^{-1}	
$E_{a,8}$	1.79×10^5	kcal kmol^{-1}	$k_8 = 2.04 \times 10^{-62}$
A_8	9.37×10^{71}	d^{-1}	
$E_{a,9}$	1.99×10^5	kcal kmol^{-1}	$k_9 = 6.24 \times 10^{-77}$
A_9	9.95×10^{71}	d^{-1}	
IMP(t=0)	3.67	mM	

Table 2: Estimated values for the parameters involved in the reaction scheme. The value of k_i computed using the estimated values of $E_{a,i}$, A_i at $T = 20$ °C is indicated in the last column.

energies are in the same order of magnitude of those reported in the literature [22]. The estimated parameters can be used, together with the storage temperature, to compute the reaction rate coefficients k_i, see Eqn (4). The last column of Table 2 shows the values of k_i at $T = 20$ °C, which is the largest temperature considered in the experiments. As shown in the table, k_2, k_4, k_5, k_8 and k_9 are close to zero which in turn suggests that the corresponding reactions are not relevant, at least in the time span of the experiments. k_i will be even closer to zero at lower storage temperatures. Based on that conclusion, a new scheme that includes only the relevant routes, as depicted in Figure 2, is proposed.

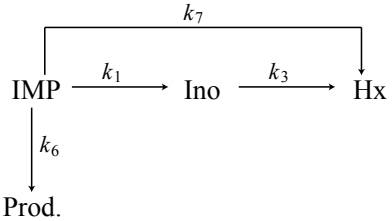

Figure 2: Postmortem degradation scheme of IMP in hake after removing the non-relevant reactions.

Figure 3 shows a comparison between model simulation results and experimental data set. Each row of figures corresponds with a different experiment. Figures at the left column show the model simulation results (continuous lines) and the experimental data (marks) for

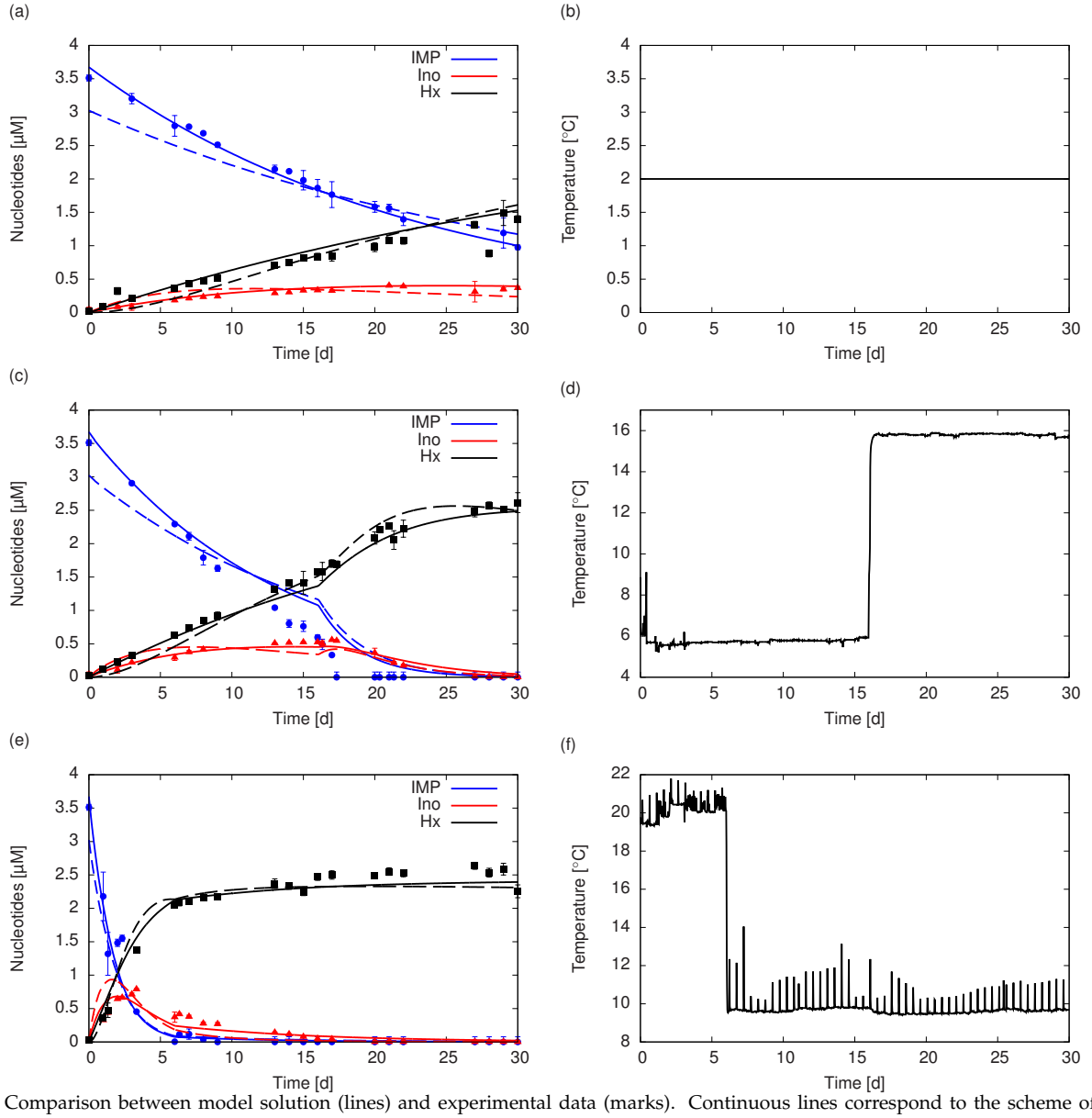

Figure 3: Comparison between model solution (lines) and experimental data (marks). Continuous lines correspond to the scheme of Figure 2 whereas dashed lines refer to the scheme of [22]. The evolution of the storage temperature in each experiment is shown in the figures in the right column.

the three nucleotide catabolites (IMP, Ino and Hx). Figures at the right column represent the storage conditions. As shown in the figure, the proposed scheme is capable of reproducing the experimental behavior with a satisfactory degree of accuracy.

In this work we have also checked the performance of the mechanistic model considered in [22], which also describes IMP degradation in fish muscle. As mentioned in the introduction, such model is a simplified version of the one proposed in this work in which k_1, k_3 and k_5 are the only reaction rate coefficients different from zero. As in the previous case, Arrhenius parameters ($E_{a,i}$ and A_i with $i = 1, 3, 5$) as well as initial conditions for IMP have been estimated from the experimental data (see Table 3). Dashed lines in Figure 3 represent the model solution using the scheme of [22]. Howgate model solution shows a slower evolution of IMP as compared with the experimental data. On the other hand, although not as evident as in the case of IMP, the fitting of Ino and Hx is not as good as in model (1)- (3).

The maximum likelihood can be used to compare the goodness of fit between different models, however it does not take into account the degrees of freedom of the system, i.e. the number of parameters to be estimated. In nested models, as the ones considered in this work, the largest value of the likelihood function will correspond with the model with the largest degrees of freedom. Nonetheless, the predictive capabilities of the largest model might be worse as they may incur in fitting data errors (overfitting). A number of methods, that pro-

Parameter	**Value**	**Units**	k [d^{-1}] at 20 °C
$E_{a,1}$	2.58×10^4	kcal kmol^{-1}	$k_1 = 0.571$
A_1	9.54×10^{18}	d^{-1}	
$E_{a,3}$	1.28×10^4	kcal kmol^{-1}	$k_3 = 0.782$
A_3	2.72×10^9	d^{-1}	
$E_{a,5}$	6.0×10^4	kcal kmol^{-1}	$k_5 = 0.067$
A_5	3.28×10^{43}	d^{-1}	
IMP(t=0)	3.02	mM	

Table 3: Estimated values for the parameters involved in the model proposed by [22]. The value of k_i computed using the estimated values of $E_{a,i}$, A_i at $T = 20$ °C is indicated in the last column.

vide a trade-off between the number of parameters and the goodness of fit, are at hand to compare models with different degrees of freedom. Among these methods, the Akaike Information Criterion (AIC) [1] seems to be more adequate [30, 15]. The AIC is defined as follows:

$$AIC = -2\log(\max L) + 2p \tag{6}$$

where $\max L$ is the maximum likelihood estimator of the likelihood function, Eq. (5), and p is the number of parameters in the model. For the largest model $p = 19$ whereas $\max L = -2088.5$. On the other hand, for the scheme of [22] $p = 7$ and $\max L = -5181.2$. Therefore, according to the AIC, model (1)-(3) is preferred.

Modifications of the AIC which may have some advantages over the AIC, see [3] and references therein for details, were tested leading nonetheless to similar conclusions.

The proposed scheme adequately describes biochemical changes in nucleotides after fish death at typical storage and transport conditions, including situations that involve the interruption of the cold chain storage. It also provides evidence on the existence of biochemical routes that seem relevant in nucleotide degradation in hake. To the best of our knowledge, such routes have not been previously reported in the context of mathematical modeling. Some of the reactions considered in the scheme of Figure 1, in particular r_5 and r_9, might become relevant after the time span considered in the experiments. However, after such period fish is already spoiled so they can be neglected for fish quality assessment purposes.

Finally, it should be remarked the interest of the biochemical model we propose to predict quality loss at the early stages of fish storage, or to improve storage or fish processing conditions. In addition, the mathematical formulation of such kinetics allows biochemical mechanisms to be combined with bacterial growth kinetics [13] or mass and heat transfer mechanisms [23] in a modular way, what expands the number of potential applications.

5. Conclusions

In this work the main biochemical routes involved in the degradation of IMP in fish at storage and transport conditions were described using a mathematical model. The proposed model reproduces the experimental measurements with a satisfactory degree of accuracy and reveals a pathway that seems relevant for nucleotide degradation at least in hake (*Merluccius merluccius*). Although the reactions involved in this pathway have been reported in earlier literature, to the best of our knowledge they have not been considered in previous mathematical models.

The study of the biochemical degradation kinetics, separately from other mechanisms such as leaching or bacterial degradation, will allow to adopt a modular approach to modeling. By combining the different underlying mechanisms on a flexible way it will be possible to develop prediction models for a varied range of scenarios, including different fish matrices, storage conditions, etc.

Future work will extend the current model to consider the influence of microorganisms on nucleotide degradation as well as mass transfer mechanisms in the food matrix.

Acknowledgements

The authors acknowledge financial support from the Spanish Ministry of Science and Innovation (Projects ISFORQUALITY AGL2012-39951-C02-01, PIE 201230E042 and RESISTANCE DPI2014-54085-JIN). We thank the reviewers for their enlightening comments.

[1] H Akaike. On a decision procedure for system identification. In *Proceedings of the IFAC Kyoto symp. on Systems Engineering Approach to Computer Control*, pages 485–490, 1970.

[2] C. Alasalvar, K. D. A. Taylor, A. Öksüz, T. Garthwaite, M. N. Alexis, and K. Grigorakis. Freshness assessment of cultured sea bream (sparus aurata) by chemical, physical and sensory methods. *Food Chemistry*, 72:33–40, 2001.

[3] A. M. Awad. Properties of the Akaike information criterion. *Microelectronics and Reliability*, 36(4):457–464, 1996.

[4] E. Balsa-Canto, V. S. Vassiliadis, and J. R. Banga. Dynamic optimization of single-and multi-stage systems using a hybrid stochastic-deterministic method. *Industrial & Engineering Chemistry Research*, 44(5):1514–1523, 2005.

[5] E. Balsa-Canto, D. Henriques, A. Gabor, and J. R. Banga. AMIGO2, a toolbox for dynamic modeling, optimization and control in systems biology. *Bioinformatics*, 2016. DOI:10.1093/bioinformatics/btw411.

[6] J. Baranyi and T. A. Roberts. A dynamic approach to predicting bacterial growth in food. *International Journal of Food Microbiology*, 23:277–294, 1994.

[7] J. M. Barat, L. Gil, E. García-Breijo, M. C. Aristoy, F. Toldrá, R. Martínez-Máñez, and J. Soto. Freshness monitoring of sea bream (Sparus aurata) with a potentiometric sensor. *Food Chemistry*, 108(2):681–688, 2008.

[8] J. Davídek, J. Velíšek, and G. Janíček. Stability of inosinic acid, inosine and hypoxanthine in aqueous solutions. *Journal of Food Science*, 37(5):789–790, 1972.

[9] S. Ehira and H. Uchiyama. Freshness lowering rates of cod and seabream viewed from changes in bacterial count, total volatile base and trimethyl amine–nitrogen and atp related compounds. *Bulletin of Japan Society of Scientific Fisheries*, 40:479–487, 1974.

[10] G. C. Fletcher and J. A. Hodgson. Shelf-life of sterile snapper (Chrysophrys-auratus). *Journal of Food Science*, 53(5):1327–1332, 1988.

[11] R. Fletcher. *Practical methods of optimization*. John Wiley & Sons, New York, 2nd edition, 1987.

[12] C. A. Floudas. *Deterministic global optimization: Theory, methods and applications*. Springer-Verlag, New York, 2000.

[13] M. R. García, C. Vilas, J. R. Herrera, M. Bernárdez, E. Balsa-Canto, and A. A. Alonso. Quality and shelf-life prediction for retail fresh hake (merluccius merluccius). *International Journal of Food Microbiology*, 208:65–74, 2015.

[14] R. Gill. Nucleotide-degrading enzymes. In N. F. Haard and B. K. Simpson, editors, *Seafood enzymes: utilization and influence of postharvest seafood quality*, pages 37–68. Marcel Dekker, Inc. New York, 2000.

[15] G. Glatting, P. Kletting, S. N. Reske, K. Hohl, and C. Ring. Choosing the optimal fit function: Comparison of the Akaike information criterion and the F-test. *Medical Physics*, 24(11):4285–4292, 2007.

[16] K. Gopakumar. Enzymes and enzyme products as quality indices. In N. F. Haard and B. K. Simpson, editors, *Seafood enzymes: utilization and influence of postharvest seafood quality*, pages 337–363. Marcel Dekker, Inc. New York, 2000.

[17] K. Grijspeerdt and K. De Reu. Practical application of dynamic temperature profiles to estimate the parameters of the square root model. *International Journal of Food Microbiology*, 101(1):83–92, 2005.

[18] K. Grijspeerdt and P. Vanrolleghem. Estimating the parameters of the baranyi model for bacterial growth. *Food Microbiology*, 16 (6):593–605, 1999.

[19] N. Haard. The role of enzymes in determining seafood color, flavour and texture. In H. A. Bremmer, editor, *Safety and Quality Issues in Fish Processing*, pages 220–253. Woodhead Publishing Limited, 2002.

[20] A. C. Hindmarsh, P. N. Brown, K. E. Grant, S. L. Lee, R. Serban, D. E. Shumaker, and C. S. Woodward. Sundials: suite of nonlinear and differential/algebraic equation solvers. *ACM Trans. Math. Softw.*, 31:363–396, 2005.

[21] H. Hong, J. M. Regenstein, and Y. Luo. The importance of ATP-related compounds for the freshness and flavor of post-mortem

fish and shellfish muscle: A review. *Critical Reviews in Food Science and Nutrition*, 2015. DOI:10.1080/10408398.2014.1001489.

[22] P. Howgate. Kinetics of degradation of adenosine triphosphate in chill-storage rainbow trout (oncorhynchus mykiss). *International Journal of Food Science and Technology*, 40:579–588, 2005.

[23] P. Howgate. A review of the kinetics of degradation of inosine monophosphate in some species of fish during chilled storage. *International Journal of Food Science and Technology*, 41:341–353, 2006.

[24] B. O. Kassemsarn, N. R. Jones, B. S. Perez, and J. Murray. Nucleotide degradation in muscle of iced haddock (Gadus aeglefinus), lemon sole (Pleuronectes microcephalus), and plaice (Peluronectes platessa). *Journal of Food Science*, 28(1):28–37, 1963.

[25] M. Kawai, A. Okiyama, and Y. Ueda. Taste enhancements between various amino acids and imp. *Chemical Senses*, 27:739–745, 2002.

[26] T. Kuda, M. Fujita, H. Goto, and T. Yano. Effects of retort conditions on ATP-related compounds in pouched fish muscle. *Food Science and Technology*, 41(3):469–473, 2008.

[27] P. T. Lakshmanam and P. Gopakumar. K-value, an index for estimating fish freshness and quality. *Current Science*, 76(3):400–404, 1999.

[28] D. P. Li, N. Qin, L. T. Zhang, J. Lv, Q. Z. Li, and Y. K. Luo. Effects of different concentrations of metal ions on degradation of adenosine triphosphate in common carp (cyprinus carpio) fillets stored at 4 ° C: An in vivo study. *Food Chemistry*, 211:812–818, 2016.

[29] K. F. Li, Y. K. Luo, and H. X. Shen. Postmortem changes of crucian carp (carassius auratus) during storage in ice. *International Journal of Food Properties*, 18(1):205–212, 2015.

[30] T. M. Ludden, S. L. Beal, and L. B. Sheiner. Comparison of the Akaike information criterion, the Schwarz criterion and the F test as guides to model selection. *Journal of Pharmacokinetics and Biopharmaceutics*, 22(5):431–445, 1994.

[31] T. Mørkøre, M. Rødbotten, G. Vogt, S. O. Fjæra, I. Ø. Kristiansen, and E. Manseth. Relevance of season and nucleotide catabolism on changes in fillet quality during chilled storage of raw atlantic salmon (Salmo salar l.). *Food Chemistry*, 119(4):1417–1425, 2010.

[32] S. Muroya, M. Oe, I. Nakajima, K. Ojima, and K. Chikuni. CE-TOF MS-based metabolomic profiling revealed characteristic metabolic pathways in postmortem porcine fast and slow type muscles. *Meat Science*, 98(4):726–735, 2014.

[33] V. M. Ocaño-Higuera, A. N. Maeda-Martínez, E. Marquez-Ríos, D. F. Canizales-Rodríguez, F. J. Castillo-Yáñez, E. Ruíz-Bustos, A. Z. Graciano-Verdugo, and M. Plascencia-Jatomea. Freshness assessment of ray fish stored in ice by biochemical, chemical and physical methods. *Food Chemistry*, 125(1):49–54, 2011.

[34] H. Okuma and E. Watanabe. Flow system for fish freshness determination based on double multi-enzyme reactor electrodes. *Biosensors & Bioelectronics*, 17:367–372, 2002.

[35] F. Özogul, K. D. A. Taylor, P. C. Quantick, and Y. Özogul. A rapid hplc-determination of atp-related compounds and its application to herring stored under modified atmosphere. *International Journal of Food Science and Technology*, 35(6):549–554, 2000.

[36] M. Palmer. Human metabolism: Lecture notes. `http://watcut.uwaterloo.ca/webnotes/Metabolism/`, June 2014.

[37] S. S. Rao. *Engineering optimization: theory and practice*. Wiley, 4th edition, 2009.

[38] M. Ruiz-Rico, A. Fuentes, R. Masot, M. Alcañiz, I. Fernández-Segovia, and J. M. Barat. Use of the voltammetric tongue in fresh cod (Gadus morhua) quality assessment. *Innovative Food Science & Emerging Technologies*, 18:256–263, 2013.

[39] T. Saito, K. Arai, and M. Matsuyoshi. A new method for estimating the freshness of fish. *Bulletin of the Japanese Society of Scientific Fisheries*, 24:749–750, 1959.

[40] T. Shiba, N. Shiraki, M. Furushita, and T. Maeda. Free amino acid and atp-related compounds in sterile tiger puffer fish (takifugu rubripes) fillets stored at 4c. *Journal of Food Process and Preservation*, 38(3):791–797, 2014.

[41] M. E. Surette, T. A. Gill, and P. J. LeBlanc. Biochemical basis of postmortem nucleotide catabolism in cod (gadus morhua) and its relationship to spoilage. *Journal of agricultural and food chemistry*, 36(1):19–22, 1988.

[42] H. L. A. Tarr. Lingcod muscle purine nucleoside phosphorylase. *Canadian Journal of Biochemistry and Physiology*, 36(6):517–530, 1958.

[43] N. Tomlinson, V. M. Creelman, and K. G. Reid. The phosphorus-containing fractions of sterile lingcod muscle during storage at 0-degrees-C. *Journal of the Fisheries Research Board of Canada*, 17(3): 371–376, 1960.

[44] H. Uchiyama and S. Ehira. Relation between freshness and acid-soluble nucleotides in aseptic cod and yellowtail muscles during ice storage. *Bulletin of the Tokai Regional Fisheries Research Laboratory*, 78:23–31, 1974.

[45] K. J. Versyck, K. Bernaerts, A. H. Geeraerd, and J. F. Van Impe. Introducing optimal experimental design in predictive modeling: A motivating example. *International Journal of Food Microbiology*, 51(1):39–51, 1999.

[46] C. Vilas, A. Arias-Méndez, M. R. García, A. A. Alonso, and E. Balsa-Canto. Towards predictive food process models: A protocol for parameter estimation. *Critical Reviews in Food Science and Nutrition*, 2016. DOI:10.1080/10408398.2016.1186591.

[47] E. Walter and L. Pronzato. *Identification of parametric models from experimental data*. Springer, 1997.

[48] L. Yao, Y. Luo, Y. Sun, and H. Shen. Establishment of kinetic models based on electrical conductivity and freshness indicators for the forecasting of crucian carp (carassius carassius) freshness. *Journal of Food Engineering*, 107:147–151, 2011.

[49] P. Zaragozá, A. Fuentes, I. Fernández-Segovia, J. L. Vivancos, A. Rizo, J. V. Ros-Lis, J. M. Barat, and R. Martínez-Máñez. Evaluation of sea bream (sparus aurata) shelf life using an optoelectronic nose. *Food Chemistry*, 138(2-3):1374–1380, 2013.

Appendix A. Experimental data

In this appendix the experimental data employed to calibrate models are presented (Tables A.4-A.6)

Time [days]	**T** [°C]	**IMP** [mM]		**Ino** [mM]		**Hx** [mM]	
		Mean	Std	Mean	Std	Mean	Std
0.0	2.0	3.51	0.04	0.04	0.04	0.03	0.00
1.0	2.0	-	-	0.08	0.00	0.08	0.00
2.0	2.0	-	-	0.08	0.02	0.32	0.05
3.0	2.0	3.20	0.08	0.08	0.05	0.21	0.00
6.0	2.0	2.79	0.15	0.18	0.02	0.36	0.03
7.0	2.0	2.78	0.01	0.21	0.02	0.44	0.01
8.0	2.0	2.69	0.02	0.23	0.02	0.48	0.01
9.0	2.0	2.51	0.03	0.24	0.01	0.52	0.02
13.0	2.0	2.15	0.06	0.29	0.00	0.71	0.01
14.0	2.0	2.12	0.01	0.30	0.00	0.75	0.01
15.0	2.0	1.98	0.15	0.33	0.00	0.81	0.01
16.0	2.0	1.86	0.13	0.33	0.02	0.84	0.05
17.0	2.0	1.77	0.19	0.33	0.02	0.85	0.07
20.0	2.0	1.58	0.08	-	-	0.98	0.06
21.0	2.0	1.56	0.06	0.40	0.01	1.08	0.03
22.0	2.0	1.40	0.09	0.39	0.02	1.08	0.05
27.0	2.0	-	-	0.31	0.15	1.31	0.05
28.0	2.0	-	-	-	-	0.89	0.05
29.0	2.0	1.19	0.23	0.35	0.02	1.49	0.19
30.0	2.0	0.98	0.03	0.37	0.02	1.40	0.05
31.0	2.0	0.93	0.08	0.36	0.02	1.41	0.05

Table A.4: Measured values (mean and standard deviation) of inosine monophosphate (IMP), inosine (Ino) and hypoxanthine (Hx) in the fish sample juice for the first experiment.

Time [days]	T [°C]	IMP [mM]		Ino [mM]		Hx [mM]	
		Mean	Std	Mean	Std	Mean	Std
0.0	8.9	3.51	0.04	0.04	0.04	0.03	0.00
1.0	5.7	-	-	0.11	0.00	0.12	0.01
2.0	5.5	-	-	0.11	0.05	0.23	0.05
3.0	5.6	2.90	0.03	0.22	0.01	0.33	0.01
6.0	5.7	2.29	0.02	0.29	0.04	0.64	0.03
7.0	5.8	2.11	0.06	0.38	0.02	0.74	0.01
8.0	5.7	1.79	0.11	0.42	0.02	0.85	0.02
9.0	5.7	1.63	0.04	-	-	0.92	0.06
13.0	5.8	1.04	0.02	0.51	0.00	1.31	0.02
14.0	5.8	0.80	0.06	0.52	0.01	1.41	0.04
15.0	5.8	0.76	0.08	0.52	0.01	1.41	0.17
16.0	9.0	0.60	0.04	0.52	0.01	1.58	0.05
16.3	15.7	0.49	0.08	0.51	0.04	1.58	0.14
17.0	15.8	0.33	0.01	0.56	0.01	1.70	0.06
17.3	15.8	0.00	0.08	0.55	0.01	1.69	0.05
20.0	15.7	0.00	0.08	0.36	0.07	2.09	0.09
20.3	15.9	0.00	0.08	-	-	2.21	0.01
21.0	15.8	0.00	0.08	-	-	2.27	0.03
21.3	15.8	0.00	0.08	0.21	0.02	2.05	0.14
22.0	15.7	0.00	0.08	0.17	0.02	2.22	0.13
27.0	15.8	0.00	0.08	0.01	0.01	2.48	0.08
28.0	15.8	0.00	0.08	0.00	0.01	2.57	0.05
29.0	15.9	0.00	0.08	0.00	0.00	2.52	0.01
30.0	15.8	0.00	0.08	0.00	0.02	2.61	0.15
31.0	15.7	0.00	0.08	0.03	0.04	2.39	0.10

Table A.5: Measured values (mean and standard deviation) of inosine monophosphate (IMP), inosine (Ino) and hypoxanthine (Hx) in the fish sample juice for the second experiment.

Time [days]	T [°C]	IMP [mM]		Ino [mM]		Hx [mM]	
		Mean	Std	Mean	Std	Mean	Std
0.0	19.8	3.51	0.04	0.04	0.04	0.03	0.00
1.0	19.4	2.18	0.36	0.33	0.01	0.36	0.01
1.3	20.1	1.32	0.32	0.44	0.02	0.47	0.11
2.0	19.8	1.48	0.05	0.64	0.02	-	-
2.3	20.4	1.55	0.05	0.66	0.02	-	-
3.0	20.5	-	-	0.71	0.02	-	-
3.3	20.8	0.45	0.00	0.79	0.01	1.38	0.02
6.0	20.1	0.00	0.00	0.37	0.08	2.05	0.05
6.3	9.6	0.11	0.00	0.42	0.01	2.09	0.05
7.0	9.7	0.12	0.08	0.38	0.02	2.11	0.05
8.0	9.6	0.04	0.07	0.28	0.02	2.16	0.05
9.0	9.6	0.00	0.08	0.27	0.02	2.17	0.04
13.0	9.8	0.00	0.08	0.14	0.01	2.37	0.07
14.0	9.8	0.00	0.08	0.12	0.01	2.33	0.05
15.0	9.8	0.00	0.08	0.08	0.00	2.24	0.05
16.0	9.8	0.00	0.08	0.05	0.04	2.47	0.05
17.0	9.6	0.00	0.08	0.04	0.00	2.50	0.06
20.0	9.4	0.00	0.08	0.00	0.02	2.49	0.02
21.0	9.5	0.00	0.08	0.00	0.02	2.55	0.06
22.0	9.5	0.00	0.08	0.00	0.02	2.52	0.05
27.0	9.6	0.00	0.08	0.00	0.02	2.64	0.05
28.0	9.7	0.00	0.08	0.00	0.02	2.53	0.06
29.0	9.7	0.00	0.08	0.00	0.02	2.59	0.09
30.0	9.7	0.00	0.08	0.00	0.02	2.26	0.10
31.0	9.6	0.00	0.08	0.00	0.02	2.26	0.12

Table A.6: Measured values (mean and standard deviation) of inosine monophosphate (IMP), inosine (Ino) and hypoxanthine (Hx) in the fish sample juice for the third experiment.